Available online at www.sciencedirect.com
SCIENCE DIRECT®
Continental Shelf Research 26 (2006) 1217–1239
CONTINENTAL SHELF RESEARCH
www.elsevier.com/locate/csr

Shallow stratigraphy and sedimentation history during high-frequency sea-level changes on the central California shelf

E.E. Grossman*, S.L. Eittreim, M.E. Field, F.L. Wong

US Geological Survey, Pacific Science Center, 400 Natural Bridges Dr., Santa Cruz, CA 95064, USA

Received 12 July 2005; received in revised form 6 February 2006; accepted 4 April 2006

Abstract

Analyses of high-resolution seismic-reflection data and sediment cores indicate that an extensive sediment deposit on the central California continental shelf is comprised of several late-Pleistocene to Holocene age facies. Offshore of the littoral zone, in water depths of 30–90 m, a 3–6 m thick veneer of fine sediment referred to as the mid-shelf mudbelt has formed along 50–100 km of the coast. The mudbelt drapes a parasequence characterized by prograding clinoforms that in places overlies a 1–3 m thick basal transgressive lag deposit. These facies overlie a prominent erosional unconformity that extends from the shore to the outer shelf. Eighteen calibrated $^{14}C_{AMS}$ ages of marine molluscs and terrestrial wood detritus sampled in cores range 15,800 yr BP to modern indicating a postglacial age for these sediments (one $>55{,}000$ yr BP represents relict sand). We model accumulation of these facies using (1) the topography of the underlying erosional unconformity interpreted from seismic reflection profiles, (2) observed sediment facies (grain size) distribution across the shelf (a proxy for wave/current sediment partitioning), and published estimates of (3) eustatic sea-level history, and (4) regional tectonics. Our model and data indicate that deposition of the transgressive lag began during early, slow postglacial sea-level rise and that a notable change in depositional environment occurred across an area of more than 200 km^2 of the outer shelf likely in response to abrupt drowning during Meltwater Pulse 1B (11,500 yr BP). We propose that rapid progradation of clinoforms may have occurred during transgression because of the unique interaction of modest rates of sediment input and tectonic uplift, variable rates of eustatic sea-level rise and a complex stepped antecedent topography. Published by Elsevier Ltd.

Keywords: Shelf; Sediment; Accumulation; Sea level; Model; Holocene; Pleistocene; California

1. Introduction

Continental shelf sediment bodies are found along many of the world's coasts (Sommerfield and Nittrouer, 1999; Swift et al., 1991) and are recognized to be important archives of large-scale coastal change. They represent one of several sinks for terrestrial and marine sediment transported to the coastal ocean and are increasingly the focus of research efforts to refine our understanding of the fate of sediment eroded from coastal settings and regional sediment budgets (Eittreim et al., 2002a, b), characterize past sea-level and climatic variability (Fernandez-Salas et al., 2003), and to better link transport processes to evolving stratigraphy (Nittrouer, 1999). Recently, it has been recognized that changes in sediment and nutrient delivery to the coast associated with human land-use activities are

*Corresponding author. Tel.: +1 831 427 4725; fax: +1 831 427 4748.
E-mail address: egrossman@usgs.gov (E.E. Grossman).

0278-4343/$ - see front matter Published by Elsevier Ltd.
doi:10.1016/j.csr.2006.04.001

contributing to extensive shoreline erosion and degradation of coastal habitats and ecosystem functions on a global scale (Hughes et al., 2003; Jackson et al., 2001). Improving our understanding of the natural variability and depositional history of sediments on the shelf therefore may help us to better assess mechanisms of sediment transport and future impacts to coastal/near-shore systems.

Shelf sediment deposition histories have largely been based on sequence stratigraphic principles originally developed for relative sea-level changes ranging 1–3 million years, considerably coarser than the millennial and glacial–eustatic frequency sea-level fluctuations (10^4–10^6 yr) relevant to this paper (Van Wagoner et al., 1988). Recent detailed studies of sedimentation along the western US margin (Columbia River, WA) (Nittrouer and Sternberg, 1981), Eel River (Nittrouer, 1999), Monterey Bay (Eittreim and Noble, 2002), and Palos Verdes (CA) (Hampton et al., 2002) have shown that significant accumulations of fine sediment formed on the shelf during the latest Pleistocene to Holocene sea-level transgression. This has led to a renewed interest in linking sediment transport mechanisms operating at the "event" (storm) and decadal/centennial scale to shoreface stratigraphy in order to predict coastal change (Frignani et al., 2005; Hampson and Storms, 2003; Harris and Wiberg, 1997; Nittrouer, 1999; Sommerfield et al., 2002; Sommerfield and Lee, 2004; Storms, 2003; Wheatcroft and Borgeld, 2000; Wiberg et al., 2002). An important gap in our understanding of coastal evolution is the role and effect of millennial-scale processes that drive large-scale coastal behavior and that have conditioned coastal environments that are now additionally impacted by human activities (Frignani et al., 2005; Neill and Allison, 2005). This paper describes the shallow stratigraphy and morphology of the central California continental shelf and examines the depositional history of a mid-shelf sediment deposit. It tests the hypothesis that a progradational clinoform wedge buried within the mid-shelf deposit formed during sea-level transgression, as a result of a dynamic interplay between an irregular stepped antecedent topography, modest sediment input, tectonic uplift, and episodic, variable sea level history.

2. Study area

This study was conducted on the central California continental shelf in northern Monterey Bay offshore of Santa Cruz (Fig. 1). The Santa Cruz shelf today is gently sloping and ~20 km wide out to

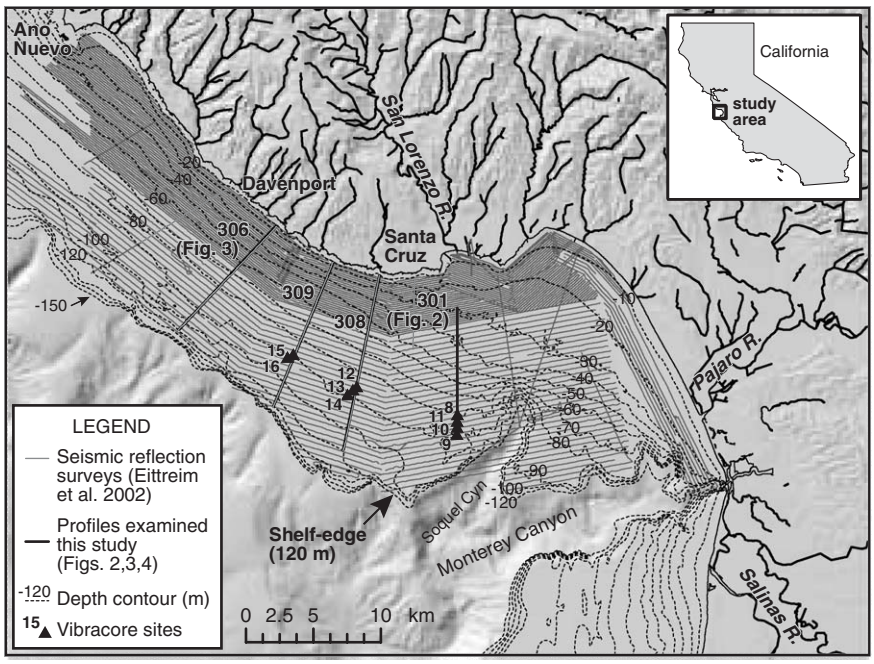

Fig. 1. Location map showing the modern, broad and gradual-sloping central California continental shelf offshore of Santa Cruz, seismic reflection profile coverage (thin lines, after Eittreim et al., 2002), select profiles (301, 308, 309, 306) analyzed in this study (solid lines), vibracore sites (solid triangles), and direction of littoral drift (arrows). Depth contours in 10-m intervals out to the shelf break.

the shelf edge at 100–120 m deep. Geologic mapping on land and seismic reflection profiling offshore indicate that the Santa Cruz coastal margin consists of Miocene to Pleistocene sedimentary rocks displaying seaward-dipping strata cut by northwest-southeast en echelon folds and faults (Eittreim et al., 2002a; Greene, 1977; Greene et al., 2002; Nagel and Mullins, 1983). These structures, and a spectacular stair-stepping succession of uplifted marine terraces northwest of Santa Cruz, are consistent with right-lateral wrench faulting typical of the broader San Andreas Fault Zone (Anderson, 1994). Radionuclide analyses show that the terraces have risen at an average rate of 1.1 mm/yr over the late Quaternary (Perg et al., 2001), higher than previous estimates ranging 0.20–0.54 mm/yr derived from amino acid racemization and alpha spectrometry uranium-series ages of molluscs (Bradley and Griggs, 1976; Kennedy et al., 1982; Lajoie et al., 1991).

The central California shelf annually receives high waves from North Pacific swell that range 1–5 m in height with 14–17 s periods between October and April. Winter storm waves periodically exceed 8–10 m and are commonly accompanied by south and southwest winds of 11–17 m/s that increase wave steepness and influence sediment transport across the inner and middle shelf. Long-period South Pacific swell that range 1–3 m (17–20 s) (National Data Buoy Center Buoy 46042) are common between June and September. This is a micro- to meso-tidal regime; the mean tidal range is ~1.1 m while spring tides range 1.6 m (http://co-ops.nos.noaa.gov/). Annual rainfall along the central California coast generally ranges 75–200 cm and increases during El Niño conditions (e.g. 1982 rainfall reached 250 cm). Northwest afternoon winds ranging 7–12 m/s blow almost daily between April and November, except during rare short-lived monsoons originating in northern Mexico/southern California. Strong northwest winds along the central California coast drive upwelling, and especially near headlands or promontories, they appear to drive currents that distribute suspended sediment and phytoplankton offshore. During winter months (November–March), wind speeds are generally lower (2.5–7.0 m/s) except during passing fronts when south and southwest winds followed by northerly clearing winds commonly blow 10–25 m/s.

Sources of sediment to the Santa Cruz littoral cell include littoral input from the north, fluvial discharge, cliff and dune retreat, and erosion of the shelf bedrock (Eittreim et al., 2002b). Littoral sediment entering from the north is estimated to be $>100{,}000\,m^3/yr$ (Best, 1990) and may reach $250{,}000\,m^3/yr$ at Santa Cruz (Best and Griggs, 1991). Fluvial discharge from the San Lorenzo, Pajaro, and Salinas Rivers is the dominant source of sediment to the coast. Together with sediment supplied from small streams, these fluvial sources contribute on average a total of $\sim 2{,}500{,}000\,m^3$ of sediment to the littoral zone each year (Eittreim et al., 2002b). Rates of coastal retreat between 1930 and 1980 determined from aerial photography of central California range 0.1–0.6 m/yr with a mean of 0.2 m/yr in the Santa Cruz Mudstone and 0.3 m/yr in the Purisma Formation (Best and Griggs, 1991). Coastal retreat supplies sediment to the littoral system at a rate of $\sim 27{,}000\,m^3/yr$ (Best and Griggs, 1991; Perg et al., 2001). Unconsolidated cliffs and dunes behind central Monterey beaches episodically retreat at rates of 2–30 m, most notably during strong El Niño events, and may be adding sediment to the littoral zone at $\sim 300\,m^3/yr$ (Thornton et al., 2003). Erosion rates of shelf bedrock exposed in the near-shore and outer shelf remain uncertain. Sediments reaching the littoral zone are partitioned. Terrigenous fine sands and silts are advected seaward and accumulate on the mid-shelf at a rate of $1.1 \times 10^6\,m^3/yr$ based on ^{210}Pb accumulation rates extrapolated over the mudbelt area (Eittreim et al., 2002b; Lewis et al., 2002). Estimates of sediment loss from the littoral system through Monterey Canyon range $\sim 250{,}000\,m^3/yr$ (Best and Griggs, 1991) to $1 \times 10^6\,m^3/yr$ (Paull et al., 2002), the latter reflecting a more comprehensive study of bed load, suspended sediment transport, and ^{210}Pb accumulation rates. Cross-shelf sediment transport is observed during winter re-suspension events (Xu et al., 2002), but the magnitude of this process and role in sediment bypassing to the slope remains uncertain. Sediment on the shelf likely escapes to Soquel Canyon, which dissects one of the thickest portions of the mid-shelf sediment deposit.

3. Methods

Seismic reflection profiles were obtained as part of the US Geological Survey Monterey Bay National Marine Sanctuary Project (Eittreim and Noble, 2002). Seismic profiles were conducted with a surface-towed 900 kJ boomer using a 1-kHz center frequency and receivers consisting of 10 and 3 m hydrophone streamers. Line spacing averaged 150 m on the inner shelf out to about 5-km offshore, and

350 m offshore (Fig. 1). The digital data were spatially filtered for swell effects by flattening to a smooth seafloor using a 24-s boxcar filter. This eliminated the effects of the dominant 5- to 7-s swell that characterized conditions during data acquisition; it had little effect on the morphology of seafloor features examined here which are generally smooth and larger than the wavelength filtered. A temporal band-pass filter of 200–800 was applied to the stacked data. Accuracy of horizon interpretations from the seismic data is about 1 m, limited by the seismic wavelength used. Differential GPS navigation provided ship-position accuracy better than ± 10 m.

Nine vibracores ranging from 0.5 to 4.5 m in length were taken at the seaward edge of the mudbelt where the thickness ranges up to 4 m (Fig. 1). Six cores penetrated silts and coarse sands to an underlying basal unconformity (see Section 4.2). Cores were analyzed for density, magnetic susceptibility, and γ-ray intensity using a multisensor core logger. Grain size was measured using a Coulter 100LS. Eighteen ^{14}C dates (Table 1) were obtained on marine carbonate shells and terrigenous wood by accelerator mass spectrometry (AMS). Marine samples were screened using a binocular microscope and subjected to a dilute 10% HCL acid etch to remove all exposed (outer) skeletal material. $\delta^{13}C$ isotope measurements accurate to (± 0.01‰) provided an additional check on skeletal alteration and were used to correct for fractionation. All dates were calibrated to calendar years using Calib-5 and are corrected for a marine reservoir age of 400 yr plus a regional correction for Northern California waters of 267 ± 19 yr (Robinson and Thompshon, 1981; Stuiver and Reimer, 1993; Stuiver et al., 1998).

Grain-size data used to characterize mean grain-size distribution across the modern shelf are derived from 2890 sample measurements compiled by the US Geological Survey usSEABED project (Reid et al., 2002). The data used in this analysis consist primarily of surface grain size measurements from box core data (Edwards, 2002).

4. Results

4.1. Shelf morphology

The central California shelf today extends between 10 and 12 km seaward from the shoreline out to an abrupt shelf break that ranges 100–120 m depth (Fig. 1). It is widest south of Santa Cruz where the shelf surrounds the head of Soquel Canyon. The shelf is generally smooth and gently inclined ($<0.9\%$). The inner shelf is covered by a thin (1–2 m) veneer of medium to coarse sand in littoral transport although 1–2 m tall outcrops of the underlying Purisma and Santa Cruz Mudstone formations are common between Santa Cruz and Ano Nuevo in water depths of 0–15 m (Anima et al., 2002; Eittreim et al., 2002a). The outer shelf is characterized by low-relief bedrock outcrops and thin sheets of relict sands and gravel (Edwards, 2002).

4.2. Pre-Holocene topography—erosion surfaces

A major angular unconformity truncates and separates the tilted Purisma and Santa Cruz Mudstone formations from overlying mid-shelf sediment deposits (Figs. 2–5). This surface is referred to herein as R1 and is correlated with a similar prominent angular unconformity in southern Monterey Bay (Chin et al., 1988). In northern Monterey Bay, R1 slopes gently in the near-shore and outer shelf but has a prominent stepped morphology in the central shelf between Santa Cruz and the Monterey Canyon. This step descends from ~42 m at the top to ~70 m at the base along seismic line 301 and grades into a rampart north of Santa Cruz. The gradient of the step (3–5%) ranges 3–5 times higher than that of the present 1% sloping inner and outer shelf.

4.3. Mid-shelf sedimentary facies

The mid-shelf sediment deposit (strata above R1) extends 50–100 km along the central California coast in water depths ranging ~30–90 m between Ano Nuevo and Monterey Peninsula; the principal deposit studied here occurs along a 50-km stretch between Santa Cruz and the Salinas River mouth (Fig. 6). It is approximately 5 km wide and reaches 30–35 m thick near the head of Soquel Canyon. Thickest sections lie just seaward of the base of the step in unconformity R1. The surface of the sediment deposit consists of fine sand and silt (Edwards, 2002) and a preliminary sediment budget indicates that it is a primary sink for fine sediment discharged by the three dominant rivers (San Lorenzo, Pajaro, and Salinas) and many small creeks entering Monterey Bay (Eittreim et al., 2002b).

Table 1
Central California mid-shelf sediment deposit ages.

Sample ID	Depth (m, msl)	Sample description	$\delta^{13}C$	^{14}C	($\pm 1\sigma$)	Cal age (kyr BP)	Cal age range (2σ) (kyr BP)	Accretion rate (mm/yr)	Notes
9-1-50	−87.5	*Macoma calcarea*	−0.025	46.49	1360	Modern	—		
10-1-223	−88.13	Slightly abraded *Macoma*	0.145	11.225	30	12.364	12.826–12.059		
11-1-362	−88.62	*Dentalium hexagonum*	1.4663	8.99	40	9.079	9.456–8.984	0.10	*,†
11-1-417	−89.17	*Nemocardium centifilosum*—pristine	0.0342	13.25	40	14.76	15.402–14.179		b
11-1-419	−89.19	*Nemocardium centifilosum*	1.1975	12.88	40	14.104	14.35–14.003		b
12-1-212A	−87.12	*Lyonsia californica*—delicate	1.265	10.535	40	11.152	11.38–10.837	0.45	**
12-1-212B	−87.12	*Macoma calcarea*	1.505	10.53	30	11.15	11.369–10.84		
12-1-340A	−88.4	*Macoma Calcarea*—juvenile	1.522	12.94	35	14.124	14.368–14.052		b
12-1-340B	−88.4	*Ensis sp.*—pristine, delicate	0.355	12.74	35	13.912	14.132–13.806		b
13-2-198	−87.98	*Macoma calcarea*—thin, delicate	−0.088	10.88	30	11.693	12.127–11.341	0.35	
13-1-340	−89.4	Wood piece (~1 cm)	−25	13.12	40	15.772	16.259–14.853		b
14-1-143	−87.43	*Crepipatella lingulata*—bryozoans	0.6343	10.91	40	11.72	12.128–11.352	0.35	†
14-1-222	−88.22	4 shell fragments	0.3681	12.97	50	14.132	14.38–14.055		b
14-1-237	−88.37	*Solen sicarius*—delicate	1.1781	13.01	40	14.212	14.402–14.077		b
15-1-125	−86.25	Whole mollusk	0.4182	10.75	40	11.381	11.747–11.104	0.16	†
15-1-171	−86.71	4 shell fragments, 1 delicate	0.4455	13.21	40	14.357	15.379–14.155		b
15-1-191	−86.91	Large shell fragments	1.9815	13.65	50	15.516	15.908–14.451		b
15-1-251	−87.51	*Macoma calcarea*	−2.7618	55.6	2500	—	—		

Sample number description: xx-x-xxx (xx = core number, x = drive interval, xxx = depth in core in cm).
d13C ($\pm$0.01‰ PDB): wood assumed −25‰.
Cal age derived using DR = 267$\pm$19 (regional mean *N.* California: Robinson and Thompson, 1981; Ingram and Southon, 1996; Berger et al., 1966).
Cal age range based on 95% probability distribution.
Notes: b = basal date; * = rate spans lithologic break and includes likely reworked sample; ** = uses mean Cal Age for samples at same depth; † = uses mean Cal Age for basal samples.

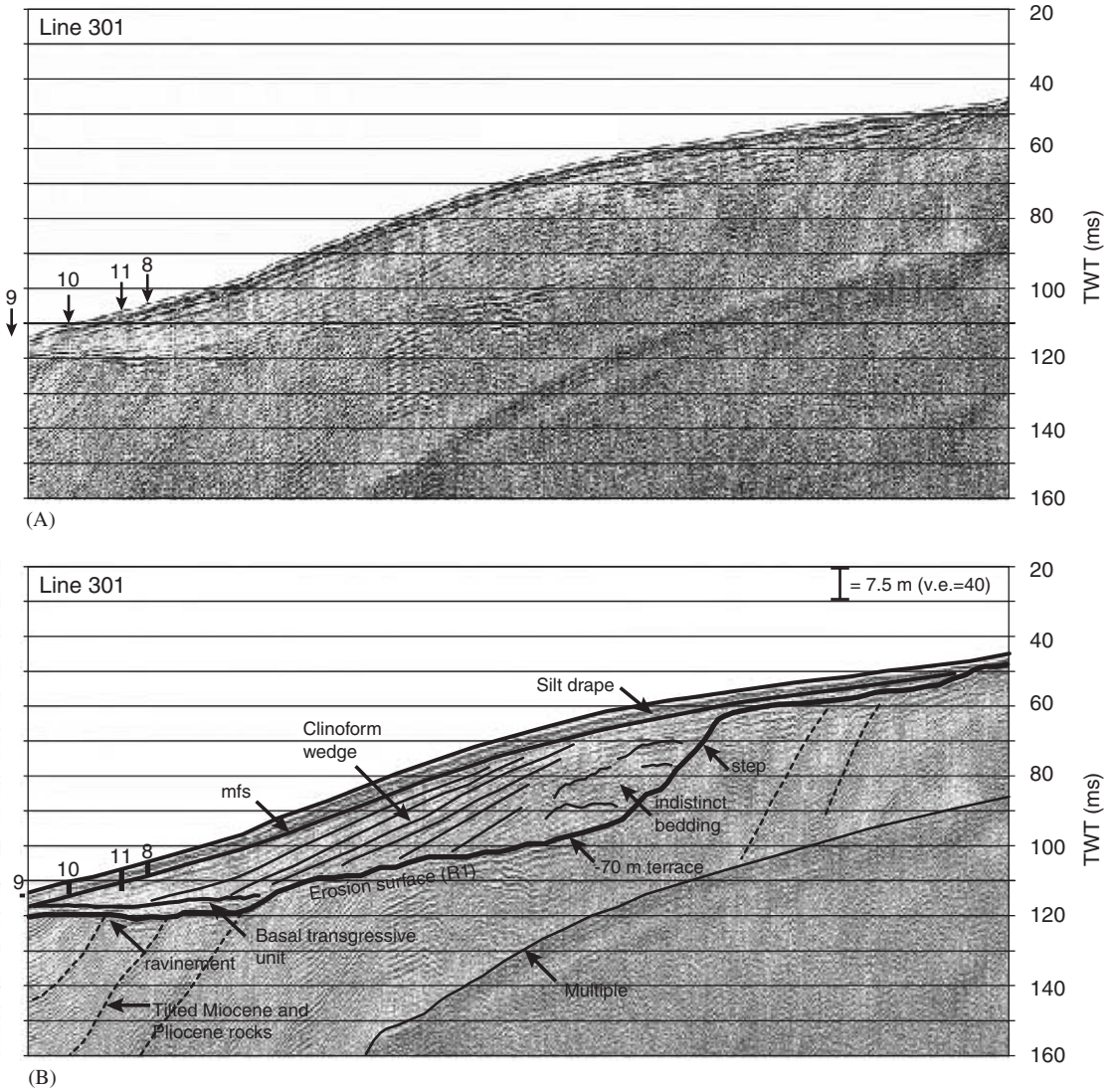

Fig. 2. (A) Uninterpreted and (B) interpreted 1 kHz boomer seismic reflection profile along transect 301 (two-way travel time in ms). (B) Shows stepped pre-Holocene erosion surface (R1), ravinement, maximum flooding surface (mfs), and three seismic facies; basal transgressive unit, clinoform wedge, and silt drape unit.

Three principal seismic facies are identified in the central California mid-shelf sediment deposit and include; (1) basal transgressive unit, (2) clinoform wedge unit, and (3) overlying drape unit (Figs. 2 and 3). The basal transgressive unit is observed only along the seaward edge of the mid-shelf and only in seismic line 301 (Fig. 2). It is characterized by flat-lying parallel to sub-parallel acoustic reflectors with moderate reflection amplitudes. It ranges 1–3 m thick. This unit differs significantly from the steeply dipping strata of the underlying bedrock (Purisma and Santa Cruz Mudstone Formations, (Eittreim and Noble, 2002; Greene, 1977; Mullins et al., 1985) and the overlying moderately dipping acoustic reflectors characterizing the clinoform wedge.

The clinoform wedge unit is characterized by regular, oblique parallel and sigmoidal, gently sloping (1–3%) reflectors that dip away from the step (Figs. 2, 3). In the central portion of the clinoform wedge off-stepping reflectors are parallel to moderately sigmoidal and extensive, while toward the step, the bedding of the clinoform unit becomes indistinct. The topsets of the inner wedge appear slightly truncated, while those of the central

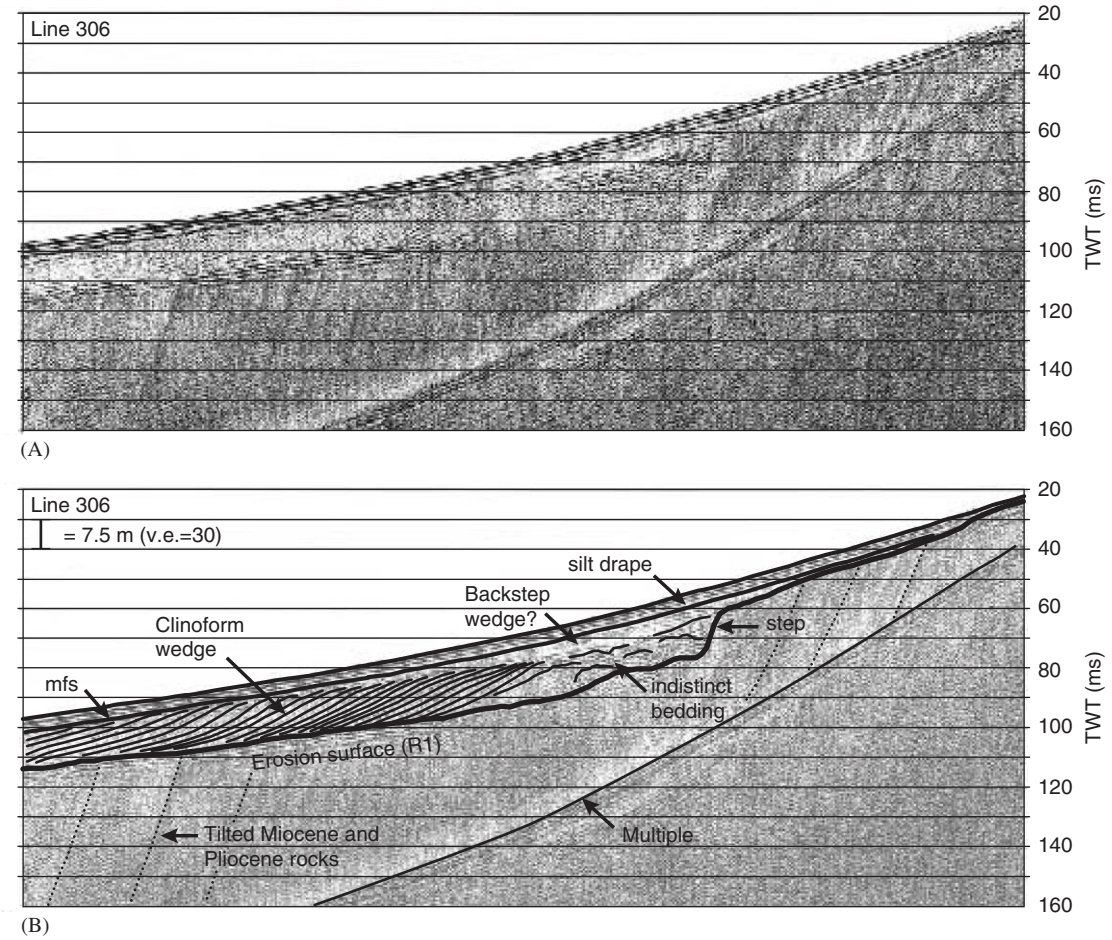

Fig. 3. (A) Uninterpreted and (B) interpreted 1 kHz seismic reflection profile along transect 306. Two-way travel time (in ms). (B) Shows stepped pre-Holocene erosion surface (R1), ravinement, maximum flooding surface (mfs), clinoform wedge, and silt drape unit.

and outer wedge show little erosion. The clinoforms downlap the basal transgressive unit on the outer middle shelf. The clinoform wedge unit extends up to 5 km across the shelf seaward from the step in R1 and reaches 15–20 m thick near the base of the step.

The overlying drape unit ranges 2–6 m thick and is comprised of horizontal to slightly oblique parallel reflectors of moderate amplitude. The drape unit overlies R1 in portions of the near-shore and outer shelf, the clinoform wedge, and basal transgressive unit.

4.4. Grain size distribution on the shelf

The modern grain size distribution on the central California shelf displays a general seaward fining trend out to the mid-shelf where a shore-parallel belt of silt and mud extends from Ano Nuevo to the Monterey Peninsula. This silt-dominated portion of the shelf is herein referred to as the mid-shelf mudbelt (Fig. 7). The mid-shelf mudbelt overlies the clinoform wedge and basal transgressive units that comprise the bulk of the sediment deposit found above R1. The littoral zone extends from the shoreline out to ~30 m depth and is characterized by rippled medium to coarse sands (Edwards, 2002; Eittreim et al., 2002a). Offshore of Santa Cruz, transitions to fine sand and to silt occur at ~25 and ~50 m, respectively.

4.5. Core samples

4.5.1. Lithology

Sediments sampled in 9 vibracores at three locations (Fig. 6) that laterally span 15 km of the outer mid-shelf mudbelt reveal similar lithology and

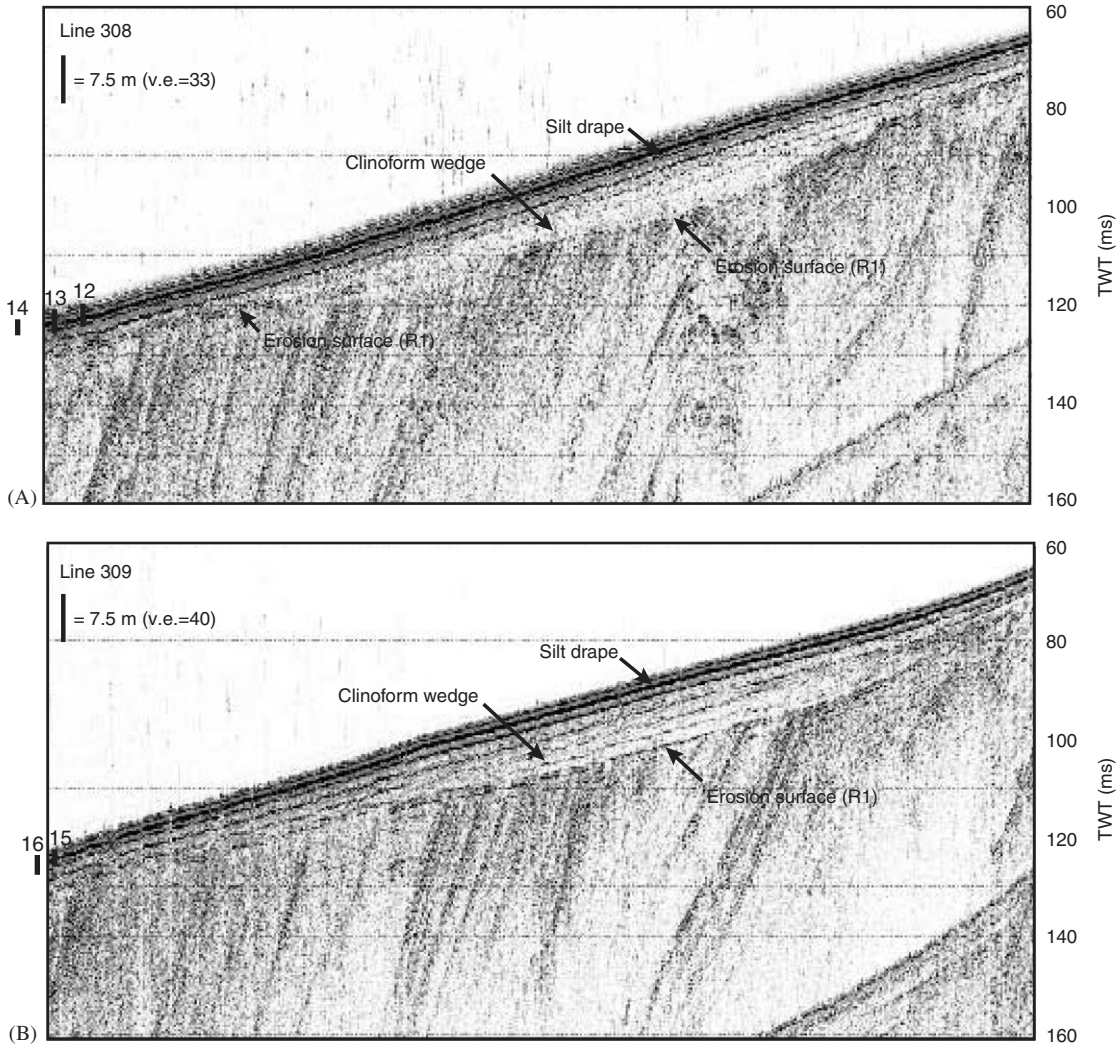

Fig. 4. 1 kHz seismic reflection profile along transect 308 (A) and transect 309 (B) showing erosion surface R1, clinoform wedge and silt drape. Two-way travel time (in ms).

stratigraphic development (five are shown in Fig. 8). Two distinct sedimentary facies characterize the seaward edge of the mid-shelf sediment deposit; a coarse basal unit and a massive silt drape unit. The coarse basal unit consists of coarse sands, pebbles and cobbles with abundant in situ and detrital skeletal material including bivalves (*Macoma calcarea, Ensis* sp., *Solen sicarius, Lyonsia californica*), gastropods (*Nemocardium centifilosum, Polinices*), and scaphopods *(dentalium hexagonum*). Although many of these have wide depth ranges (0–500 m), *Macoma* are more abundant in shallow-shelf regions and *Lyonsia californica* are most common in muddy, low-energy settings including embayments (Smith and Carlton, 1975). Several shells used for dating (Table 1) are clearly reworked (14-1-222, 15-1-171, 15-1-191), other more delicate and minimally abraded shells (12-1-212A, 12-1-340B, 13-2-19814-1-237) appear to have been rapidly buried or spent little time in transport. Terrestrial (wood) debris also occurs in this facies. The mean grain size of the matrix supporting the coarse fraction of the basal unit ranges 0.10–0.15 mm (Fig. 8(B), core 14). We interpret this basal unit as a shallow marine facies based on the abundance and preservation of shell material and coarse grain size.

The massive silt drape unit overlies the shallow-marine facies and consists of featureless, massive silt

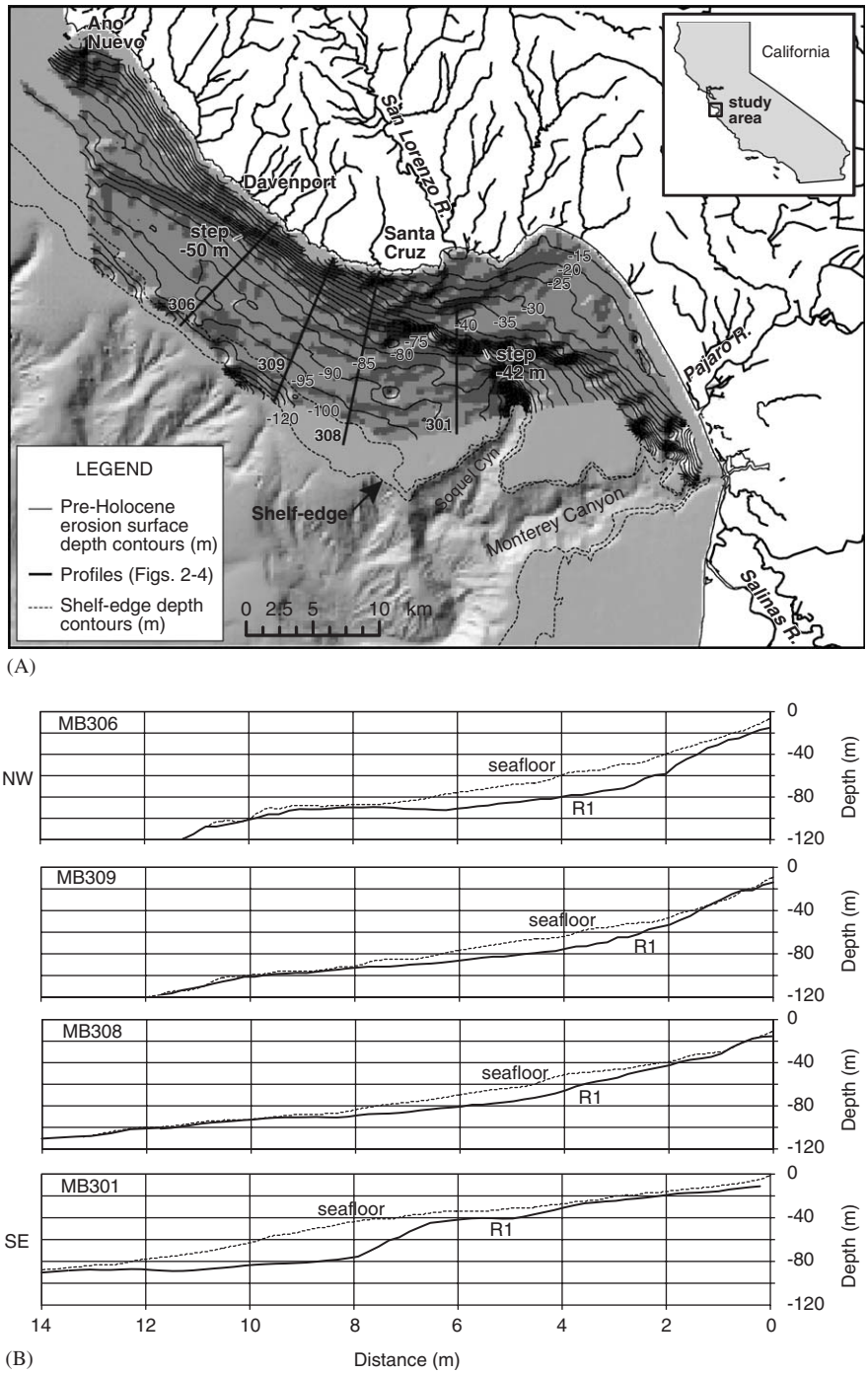

Fig. 5. (A) 200-m gridded elevation of pre-Holocene erosion surface (5-m depth contours (solid lines) displaying erosional step offshore of Santa Cruz between −40 and −70 m. Shelf edge contours −100 and −120 m (dotted lines). Seismic profiles (Figs. 2–4) for reference (bold dotted lines). (B) Cross-shore profiles of erosion surface (R1) and modern seafloor bathymetry showing step in erosion surface R1 offshore of Santa Cruz (Line 301) and 10–20 m thick mid-shelf sediment deposit.

and sandy-silt. Skeletal fragments are largely absent or <0.05 mm in size. The mean grain size of this facies ranges 0.03–0.05 mm (Fig. 8(B), core 14) and is slightly smaller in the middle portions of the unit relative to the top and contact with the underlying shallow-marine facies. Small (0.5–1.5 mm)

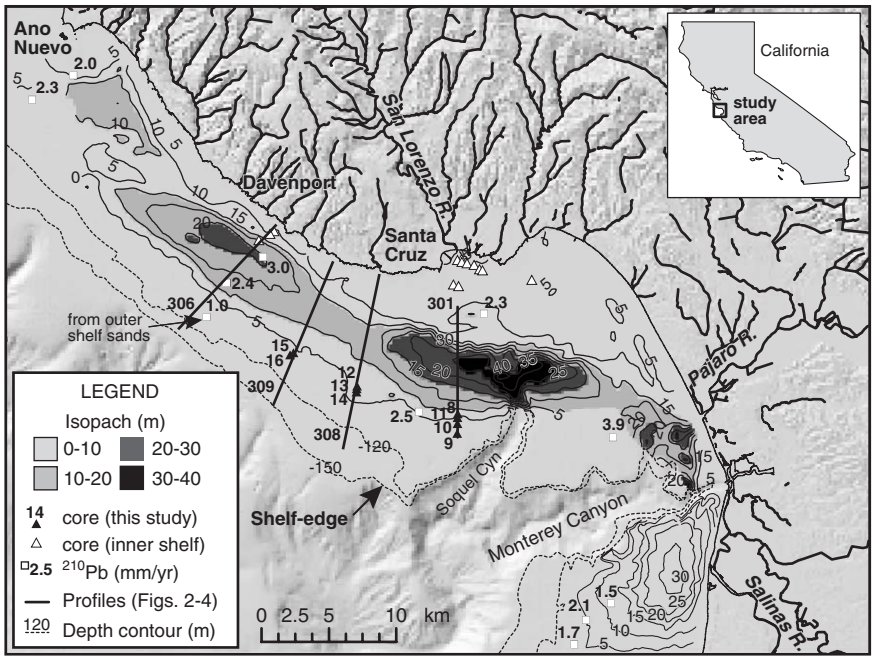

Fig. 6. Mid-shelf sediment deposit thickness (5-m isopach contours, thin solid lines), vibracore sites (solid triangles), and ^{210}Pb accumulation rate determinations (open boxes, after Lewis et al., 2002). Shelf edge contours (dotted lines) and seismic profiles analyzed (bold dotted lines) for reference.

aggregates of silt are infrequently dispersed throughout this facies and are presumed to be bioturbated and biologically reworked pelloids bound by organic matter.

4.5.2. Geochronology

Articulated or extremely delicate bivalves (Samples 11-1-417, 11-1-362, 12-1-212A, 13-2-198, 14-1-237, 15-1-125, 15-1-171, Table 1, Fig. 8) including *Macoma calcarea, Ensis* sp. (razor clam), gastropods, and scaphopods *(dentalium hexagonum)*, some in tact, are presumed to be in growth position or have experienced little transport. Other small (juvenile) clams (sample 12-1-340A) are thought to have experienced rapid burial. The age of one wood sample (13-1-340) is consistent with ages of marine shells at comparable basal depths among the four vibracores (11, 12, 13, 14, 15).

The ages of marine skeletal material and terrestrial wood at the base of cores 11, 12, 13, 14, and 15 range between 14.08 and 15.77 ka, indicating that deposition of the basal unit began sometime after ~14–15 ka and accumulated until 11.15–12.36 ka across >15 km of the outer mid-shelf. One shell found at the base of core 15 dated >55,000 ^{14}C yr and is presumed to correlate with relict sands of similar age (Edwards, 2002). One abraded, fractured, and likely reworked shell in core 15 was subsampled slightly above the basal shallow-marine facies and is 11.38 ka. Only one datable shell was found in the overlying massive silt-drape at 50-cm below the surface (9-1-50) and it was composed of modern carbon.

Vertical sediment accumulation rates based on the measured ^{14}C ages of the basal unit range 0.1–2.0 mm/yr and average 0.3 mm/yr (Table 1). Applying the core-specific accumulation rates up through each section provides an estimated maximum age of the lithologic contact at the top of the basal shallow-marine facies. The calculated age of this lithologic contact ranges 11.22–12.62 ka for cores 12, 13, 14, 15 (Fig. 8(B)). A single date of 12.36 ka at the top of the basal unit and immediately below the contact in core 10 may also be consistent with this accumulation history.

5. Discussion

5.1. Origin of erosion surface (R1)

Fig. 9 illustrates the relationship of the erosion surface (R1) and overlying mid-shelf sediment facies

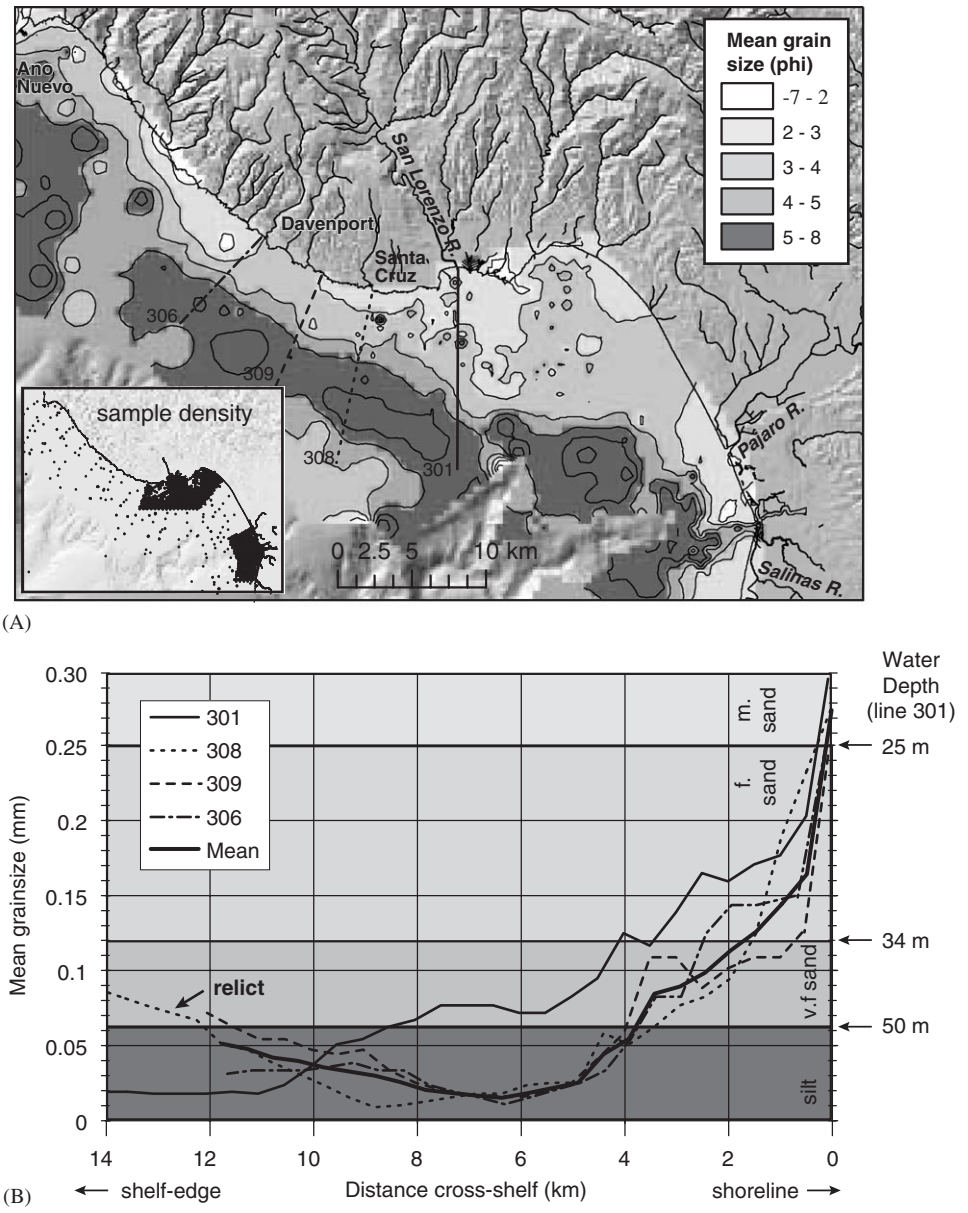

Fig. 7. (A) Map of 500-m 12-near-neighbor gridded mean grain size of shelf surface sediment (contours in 1 phi). (B) Cross-shore profiles of mean grain size along line 301 (sold line), 308 (dotted line), 309 (dashed line), 306 (dotted dash line) showing depth of transition from medium sand to fine sand (−25 m), fine sand to very fine sand (−34 m) and very fine sand to silt (−50 m) along line 301. Also shown is the mean grain size profile of 308, 309, and 306 (bold solid line). A clear partioning of sediment occurs on the central California shelf with silt and mud deposited along a mid-shelf mudbelt while sands occur in the near-shore and relict gravels (Edwards, 2002) exist on the outer shelf edge.

along seismic line 301 to the postglacial eustatic sea-level history of Bard et al. (1990). The eustatic sea-level curve was registered to the cross-shore profile by fixing the modern position of sea level to an elevation of 0 at the present time and the Last Glacial Maximum (21 ka) position of sea level (−120 m) to the −120 m depth found today near the shelf break. Also shown with the two, hatched bands are the depth zones impacted by Meltwater Pulses (MWP) 1A and 1B, episodes of abrupt

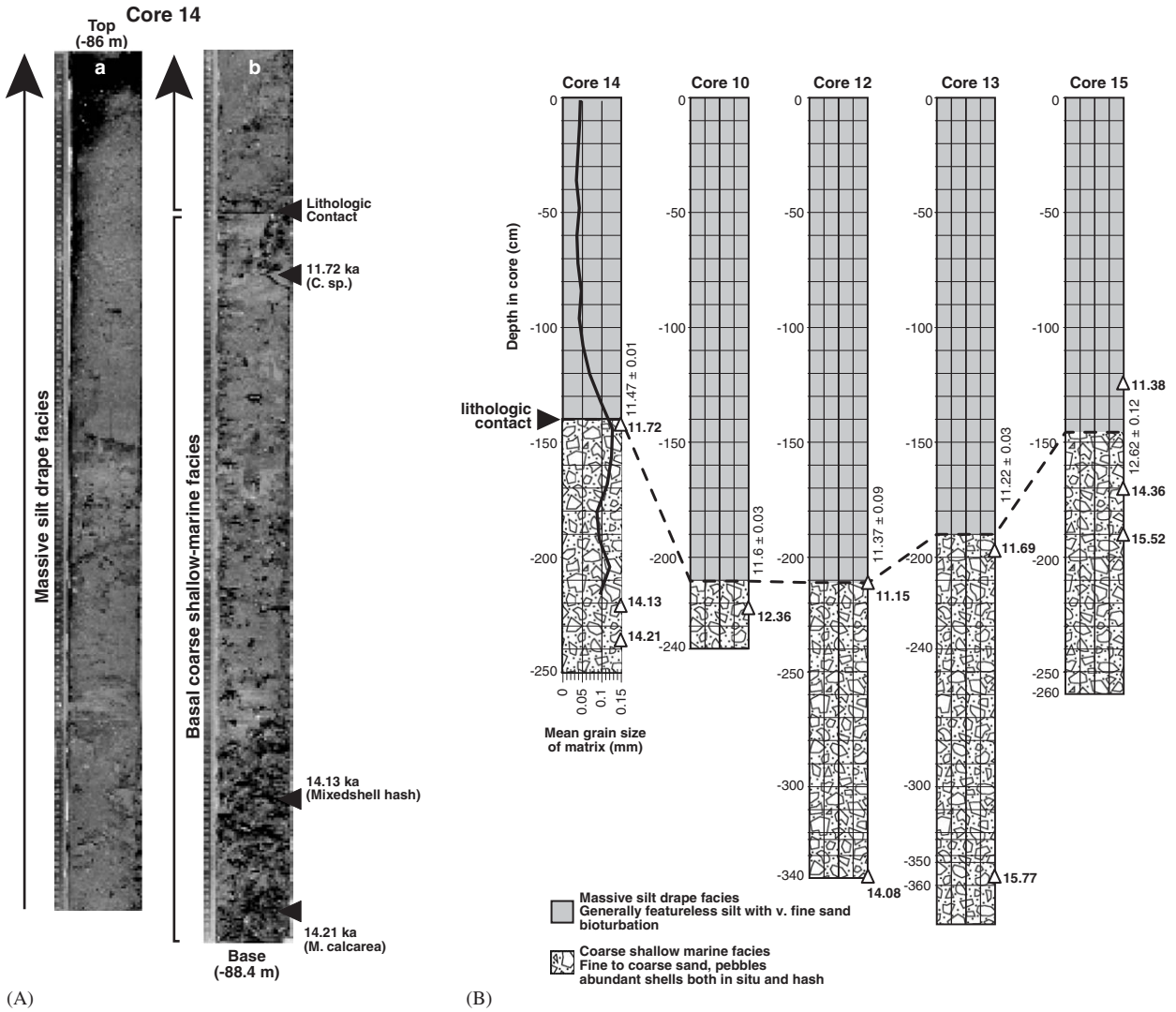

Fig. 8. (A) Core 14 photograph (representative of seaward mudbelt cores) showing basal coarse shallow-marine facies rich with detrital shell and wood, in situ articulated molluscs, and fine to coarse sands and gravels underlying massive silt drape displaying occasional mud clumps. ^{14}C dates samples (solid triangles) and depth of lithologic contact between well-sorted fine silt drape and basal poorly sorted coarse shallow-marine unit. (B) Stratigraphic diagrams of cores from three sites along >15 km of seaward mudbelt edge. Mean grain size of matrix (in mm) shown for core 14 (solid line), ^{14}C dated samples (triangles, in 1000 yr BP), lithologic contact (dashed line) and associated age (vertical text, with 2σ error) based on ^{14}C-derived accumulation rates (see Table 1). The age of contact in each core (except core 15) centers around 11.5 ka coincident with drowning during Meltwater Pulse-1B.

sea-level rise owing to rapid transfer of glacial ice and proglacial lake water to the oceans (Fairbanks, 1990).

We interpret the ubiquitous strong acoustic reflector (R1) found at the base of the mid-shelf sediment deposit (Figs. 2–5, 9) as the Pleistocene-Holocene erosion surface. It correlates to the Pleistocene–Holocene erosion surface described elsewhere on the central California shelf (Chin et al., 1988; Greene, 1977; Mullins et al., 1985). We consider the step found between ~40 and 70 m below modern sea level to be formed by terrace cutting and coastal retreat during the early post-glacial transgression 21–12 ka. During this time rates of sea-level rise were relatively lower and matched rates of uplift along the central California Coast (~1 mm/yr, (Perg et al., 2001)), which is illustrated by the strong correlation between the

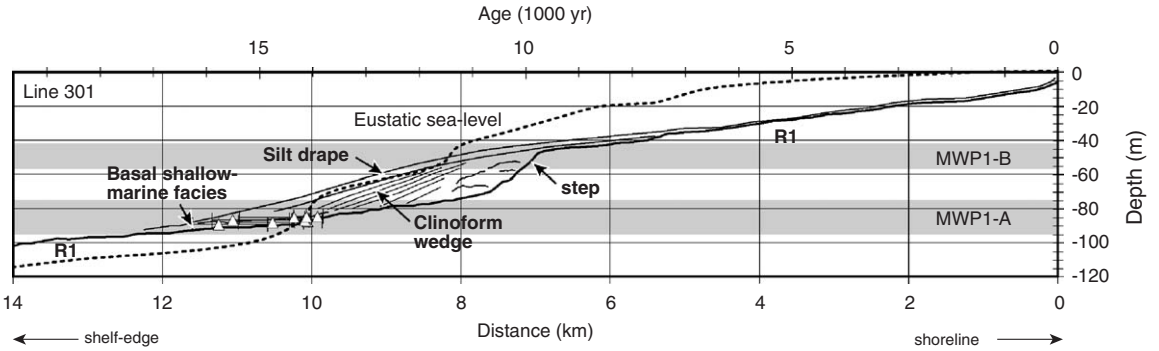

Fig. 9. Reconstruction of mid-shelf sediment deposit accumulation history with respect to erosion surface (R1) and postglacial eustatic sea-level history. Sea-level curve is registered to the cross-shore profile (301) by fixing the modern position of sea level at 0-m elevation at the present time and the Last Glacial Maximum (21 ka) position of sea level (−120 m) to the −120 m depth found today at the shelf break. A correction for at least 0.8 mm/yr uplift is required to plot ^{14}C-dated samples from basal shallow-marine unit (open triangles with 2σ uncertainty ranges) below sea level (see discussion).

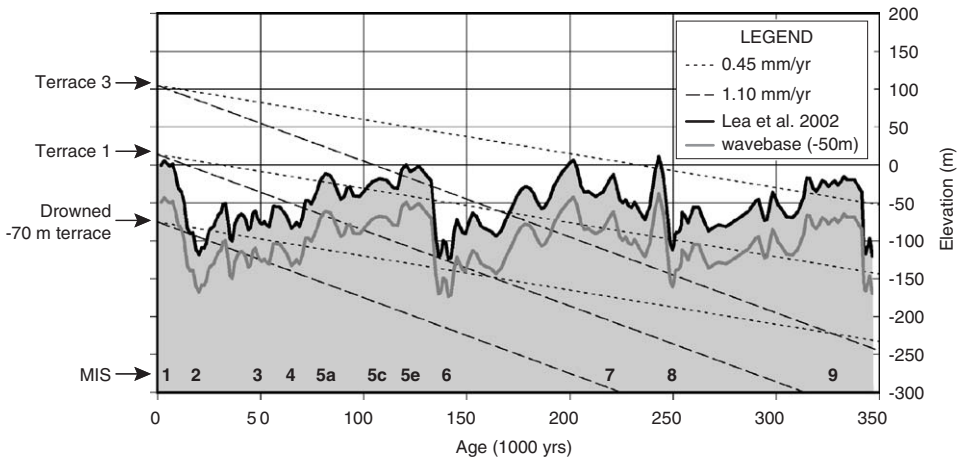

Fig. 10. Possible uplift histories and times of wave abrasion of emergent Santa Cruz marine terraces 1 and 3 (Perg et al., 2001) and drowned −70 m terrace (this study) relative to late Pleistocene eustatic sea-level history.

cross-shore shape of R1 and postglacial sea-level history (Fig. 9).

5.2. Constraints on regional uplift rate and marine terrace origins

Based on our understanding of regional uplift and eustatic sea-level history, only select periods of time in the recent past were favorable for erosion of R1; portions of MIS 6, MIS 3, and MIS2/1. Fig. 10 illustrates the range in uplift of the prominent emergent Santa Cruz terraces (Terrace 1 and 3 of Perg et al. (2001)) and the −70 m terrace found along R1 in this study relative to the Lea et al. (2002) model of late-Pleistocene eustatic sea level. The two uplift histories reflect two different uplift rates; 0.45 mm/yr (upper value of previous estimates (Bradley and Griggs, 1976; Kennedy et al., 1982; Lajoie et al., 1991)) and 1.1 mm/yr after (Perg et al., 2001). Wave base delineated 50 m below the sea-level curve shows the depth of sand movement and scour through time and is based on measurements of near-bed shear stresses that transport sand on the shelf (Storlazzi and Jaffe, 2002; Xu et al., 2002) and observations in this study of the grain size transition of sands and silts at −50 m (Fig. 7).

Marine terraces and sea cliffs form primarily through wave and sediment abrasion during stable sea level, although bioerosion and chemical

weathering can also be important (Anderson et al., 1999; Sunamura, 1992). Low rates of sea-level rise result in the formation of terraces and notches (Sunamura, 1992), while high rates of rise or fall encourage preservation through rapid submergence or emergence as the depth and location of abrasion quickly migrates across the shelf (Fletcher and Sherman, 1995). Over millennial time scales, wave abrasion associated with sea level may reoccupy specific settings and reshape shelf morphology.

At the lower uplift rate of 0.45 mm/yr (Fig. 10), the emergent Terraces 1 and 3 would have been susceptible to wave-related erosion processes during the last three sea-level highstands, whereas at the higher rate of 1.1 mm/yr, wave erosion would be largely limited to the period since the middle MIS 6 (Fig. 10). The ^{10}Be and ^{26}Al ages of the Santa Cruz marine terraces constrain the duration of exposure of emergent beach deposits that have accumulated on them and indicate a MIS 3 and 5e origin for Terraces 1 and 3, respectively (Perg et al., 2001). The higher (1.1 mm/yr) uplift rate derived from these terrace ages would greatly enhance the preservation of the terrace features by rapidly raising the unconsolidated deposits out of the influence of wave scour during subsequent sea-level transgressions which are thought to remove significant portions of such shelf deposits from the geologic record (Trincardi and Field, 1991).

At the lower uplift rate of 0.45 mm/yr, erosion processes available to cut the −70 m terrace and step of R1 existed during portions of MIS 6, MIS 4-2 (~70–~25 ka), and again during the early postglacial transgression (Fig. 10). If R1 formed prior to the Last Glacial Maximum, then wave processes associated with early postglacial transgression and the reduced rates of sea-level rise during the Younger Dryas, would have likely reshaped different sections of it and the step (Fig. 9). At the higher uplift rate, however, this terrace would have experienced wave base processes only since MIS 3 and MWP-1A and MWP-1B would have helped preserve the mid-shelf step morphology in R1, as the depth of wave scour jumped abruptly above the top of the step (Fig. 9). Moreover, the low rates of sea-level rise that typify the early and late postglacial transgression likely helped to shape the uniformly low-sloping parts of R1 on the outer and inner shelves, respectively, as relative stability or slight sea-level rise would have dominated if uplift was close to the 1 mm/yr rate rather than the lower value.

At coastal retreat rates observed during this century (0.3–0.6 m/yr, Hapke, pers. commun. 2005), the erosion surface (R1) along the outer and inner shelves (each about ~6 km wide along Line 301) could have formed in 10,000–20,000 years, since the Last Glacial Maximum (21 ka). Rates of retreat were likely higher in the past 10–20 millennia in mid-shelf depths for two reasons; (1) shallower (more energetic) conditions existed across the shelf until about 6–8 ka, and (2) wave power reaching the shore was likely higher before the inner shelf widened and the shoreface equilibrated with sea-level stability and the dominant wave regime. In summary, the geometry and correlation of cross-shelf morphology with postglacial sea-level history, measurements of wave scour, knowledge of coastal retreat rates, and our understanding of shelf sediment preservation lend support that the erosion surface R1 formed largely under postglacial sea-level rise and a regional uplift regime consistent with dated emergent marine terraces.

5.3. Postglacial origin and preservation of mid-shelf sedimentary facies

Our ^{14}C-derived ages indicate that the basal shallow-marine shell-rich unit observed in our vibracores began forming ~14–15 ka (Figs. 2, 8, 9). A single basal age greater than 55,000 ^{14}C yr BP from core 15 indicates this basal unit may directly overlie a unit of relict sands observed elsewhere on the outer shelf (Edwards, 2002). Assuming the cored basal unit is correlative to the basal unit observed in seismic reflection (i.e. along Line 301), then it predates the overlying clinoform wedge and a model of trangressive clinoform development (Cattaneo and Steel, 2003) subsequent to ~14–15 ka is likely. An alternative scenario is that the basal sediments sampled in our vibracores comprise the seaward margin of the clinoform wedge itself. This relationship would indicate a low-stand (MIS 2) or regressive (MIS 3) origin with final accumulation of the clinoforms occurring between 15 ka (base of dated coarse unit) and ~11.5 ka (top of dated coarse unit). We acknowledge that the mid-shelf deposit has characteristics of a regressive feature (Trincardi and Field, 1991). However, because of its modern depth, geometry, preservation, and tectonic and accumulation history, we believe it is more likely that the mid-shelf deposit is younger than MIS 2/3 and representative of a transgressive parasequence similar to those reviewed in Cattaneo and Steel

(2003) and Labaune et al. (2005) through advection–diffusion processes similar to those described by Pirmez et al. (1998). In addition, core logs noting penetration to the underlying bedrock suggest that the basal shallow-marine facies in our core samples correlate with the basal transgressive unit interpreted in seismic reflection profiles. The ages determined from the basal samples in our cores then constrain the deposit to a postglacial age.

If our dated samples represent the age of sediments from the seaward edge of the clinoforms and not of a distinct basal unit below it, then they indicate that initial clinoform development near the inflection point in R1 (now at −50 to −75 m) began earlier than 14–15 ka. Prior to 15 ka, sea level was below ~100 m (Fig. 10) and 10–35 m below the inflection point in R1 and the landward margin of the clinoform wedge. These conditions would point to a subaerial origin for at least the landward portion of the clinoform unit, similar to shelf-edge deltas described elsewhere (Suter and Berryhill, 1985). Our seismic reflection data do not show evidence of a transgressive surface of erosion within the clinoform wedge or a change in sedimentary facies within our core samples owing to a transition from subaerial to marine sedimentation. A more likely origin for the mid-shelf sediment deposit is postglacial accumulation.

Although many examples exist of clinoform development during sea-level regression (Trincardi and Field, 1991), the likelihood for their preservation following subsequent transgression along the energetic central California coast is low, unless they are lithified or cemented (which incidentally is not observed among the emergent Santa Cruz marine terrace sediments). From a sediment budget point of view, the scenario that only the silt drape is postglacial produces a significant discrepancy between modern and past accumulation rates, given the relatively high modern rates of sediment delivery to the coast (Best and Griggs, 1991; Perg et al., 2003), high accumulation on the mid-shelf (Eittreim et al., 2002b; Lewis et al., 2002), and the suggestion that historical rates of sediment delivery to the coast have increased significantly due to human land-use activities (Paull et al., 2002).

The delicate and articulated nature of several molluscs found in or approximating growth position at the base of our cores (11-1-417, 12-1-212A, 12-1-340B, 13-2-198, 14-1-237, 15-1-171) suggests that reworking was minimal and/or that burial (preservation) was rapid. It is apparent from Fig. 9 that several of the marine-carbonate samples plotted (11-1-417, 14-1-222, 14-1-237, 15-1-171, 15-1-191) require a significant (4–15 m) correction for uplift in order to originate below sea level. This adjustment of sample depth to paleo-sea-level position is consistent with an uplift rate of at least 0.8 mm/yr. An additional correction for ~10 m water depth corresponding to modern depths where fine to coarse littoral sands occur (Fig. 7) and where similar invertebrates are abundant on the shelf today (Smith and Carlton, 1975) necessitates a ~1 mm/yr uplift rate in agreement with the radionuclide-derived rates for marine terrace emergence (Perg et al., 2001). In any event, the basal ages measured are maximum ages for the unit and therefore accumulation rates (Table 1) derived from them are minimum rates.

5.4. Depositional model for the mid-shelf sediment deposit

Based on the radiometric dating of cored sediment across >15 km of the outer shelf (Figs. 1 and 8) and interpreted stratigraphic relationships (Figs. 2–4), initial development of the mid-shelf deposit began shortly after 14–15 ka with the accumulation of the basal shallow-marine facies when sea level was between 90 and 100 m below present (Fig. 11(A)). Between 14.5 and ~12.0 ka, despite rapid sea-level rise associated with MWP-1A, the outer shelf was characterized by water depths of 5–20 m and presumably moderate to high energy (similar to the modern wave regime of the inner shelf). It is during this time that the basal shallow-marine unit was deposited; this unit may be the landward extent of coarse relict sediment observed near the shelf edge today (Edwards, 2002). The downlap of the clinoforms onto the basal unit and our ^{14}C dates from the uppermost portion of the basal unit place a maximum age on the clinoform wedge of ~12–11 ka (Figs. 2, 9, 11(A)).

We propose that the origin of the clinoform wedge is linked to unique depositional processes as sea level inundated the stepped antecedent topography along this particular coast between 11 and 6 ka. The geometry and internal structure of the wedge is similar to those of postglacial shelf-phase and shelf-edge deltas described along the US Gulf coast (Suter and Berryhill, 1985), Southern Washington–Northern Oregon (Twitchell and Cross, 2001), and recently off of Cadiz, Spain

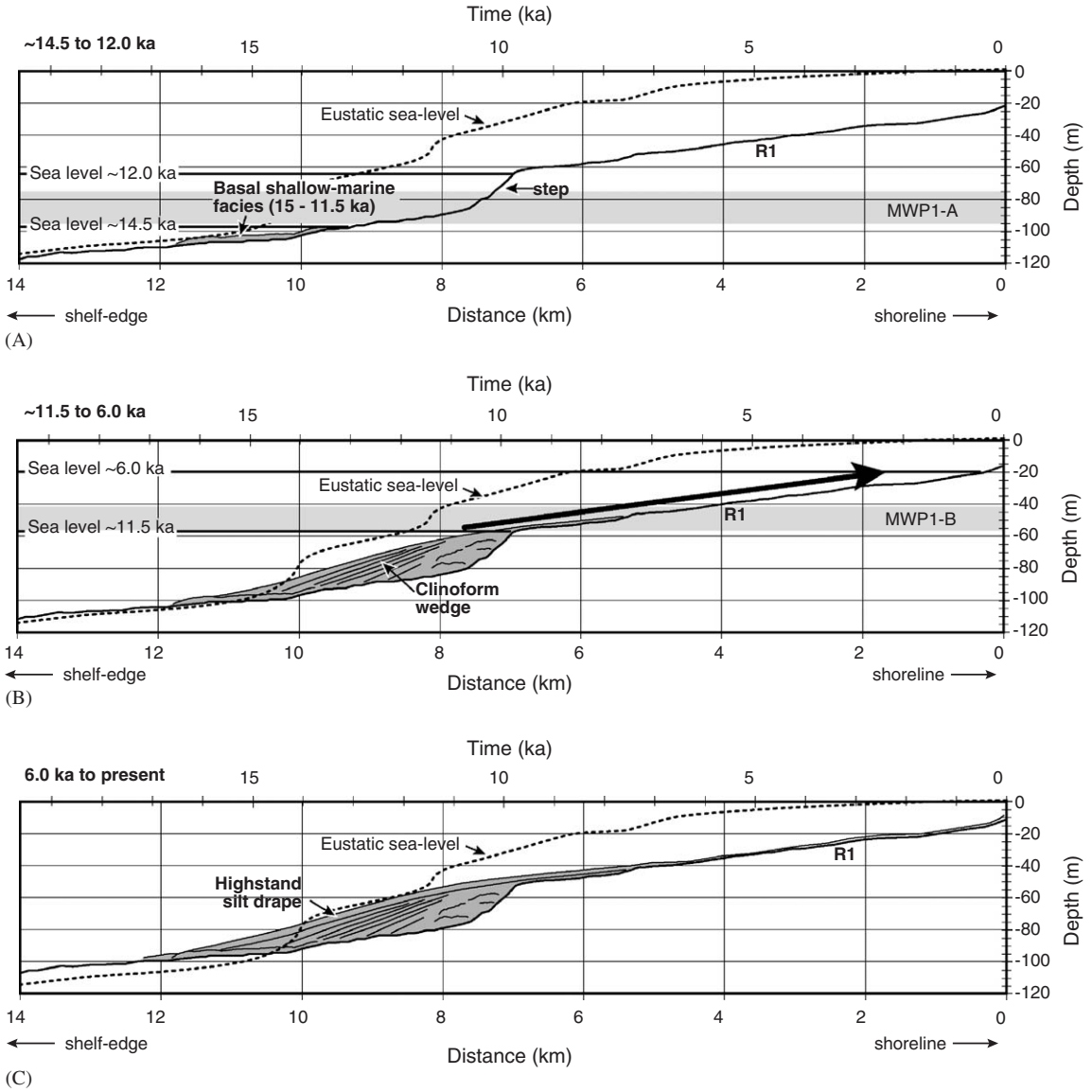

Fig. 11. Model of 3-phase sedimentation history. (A) Between 14.5 and 12.0 ka (during MWP-1A and just prior to MWP-1B) sea level floods the outer shelf, which is characterized by shallow, energetic seas fronting and eroding the step in R1 erosion surface. Coarse sediments rich with shell material deposit as transgressive lag on outer shelf and toward base of step. (B) Abrupt sea-level rise of MWP-1B rapidly drowns outer shelf settings and over-tops the step in R1 as the shoreline backsteps 2–3 km landward. The inner shelf becomes a shallow high-energy setting for 5000 yr and sediments delivered to it are transported offshore of the erosional step in the form of prograding clinoforms where adequate accommodation space exists. (C) From 6.0 ka to present, highstand conditions lead to draping of the entire mid-shelf sediment body with fine silts and mud.

(Fernandez-Salas et al., 2003) and the Rhone Delta (Labaune et al., 2005). It may represent the first of a landward-stepping transgressive parasequence of the T-C2 or T-D type of Cattaneo and Steel (2003) that are characteristic of settings with complex antecedent topography and/or high-gradient, and modest sediment supply (a second backstepping progradational unit may have occurred but is only preserved along Line 306, Fig. 3(B)).

Today, fine to very fine sands are found between ~25 and ~50 m in water depths beyond active littoral drift but shallower than depths of silt accumulation (Fig. 7). Assuming near-bed shear stresses associated with waves and currents in the

past were similar to today, deposition of similar size materials that comprise clinoforms would occur in water depths less than ~50 m or shallower settings protected from comparable wave exposure. It is likely that during abrupt sea-level rise of Meltwater Pulse 1B (~11.5 ka) the shoreline transgressed rapidly landward (2–3 km) above the top of the step in R1 producing shallow energetic conditions that promoted transport of fluvial-derived sediment offshore of the inner shelf (arrow, Fig. 11(B)) through advection–diffusion processes and sediment by-pass across the shelf (Pirmez et al., 1998). Between 11 and 6 ka, the only adequate accommodation space for the sand-size fraction of sediment input by the area's rivers existed seaward of the step in R1; a setting ideal for the accumulation of sediment and formation of clinoforms. Sediment by-pass would help to explain the slight truncations of the topset structures that are more apparent near the step rather than the seaward edge of the clinoforms.

We interpret the silt drape facies displaying internal upward coarsening sediments (Fig. 8; also see Edwards, 2002) as part of the highstand system tract (Fig. 11(C)). A modern ^{14}C-derived age of shell buried at 50 cm reflects modern physical and/or biogenic mixing to this depth, which is slightly deeper but consistent with ^{210}Pb analyses (Lewis et al., 2002) that suggest modern processes and sediment contribute to the mudbelt. The contact between the silt drape and underlying clinoform wedge and basal units is interpreted as a maximum flooding surface (Fig. 2). The draping of silt size sediment over pre-existing substrates since eustatic sea level stabilized (~6 ka) across depths of ~85 m is consistent with its accumulation today through across- and along-shore (northwestward) suspension and advection processes (Storlazzi and Jaffe, 2002; Xu et al., 2002). The dominant sources for this silt fraction are thought to be the San Lorenzo, Pajaro and Salinas Rivers and the numerous small, high-relief coastal streams that together discharge $>2.5\times10^6\,m^3$ of sediment to the coast each year (Eittreim et al., 2002b).

5.5. Clinoform development and sediment budget

To test the validity of this postglacial reconstruction and whether the volume of sediment input needed to form the clinoform wedge during transgression (11–6 ka) is consistent with inputs observed along the central California coast, we compare the rate of sediment addition needed to produce the clinoform wedge with the regional sediment budget. Based on the average clinoform wedge thickness of 15 m and average cross-shore length of 5 km, the volume of sediment needed annually to form the clinoform wedge along the 50-km area offshore of Santa Cruz over 5000 years (11–6 ka) is 750,000 m^3. This value is comparable to the 780,000 m^3 of littoral sand input annually to the shelf from all sources not including littoral inputs from the north, which are thought to escape the shelf through Monterey Canyon (Eittreim et al., 2002b). This suggests that clinoform development between ~11 and 6 ka does not require an unreasonable sediment supply, but in fact one similar to that observed today. In addition, sediment delivery to the coast may have been greater between 11 and 6 ka due to wetter early Holocene climate following the Younger Dryas (~12 ka) as observed in the Southwest (Liu et al., 2000; Rhode, 2002) similar to wet El Niño conditions today (Hicks and Inman, 1987; Inman and Jenkin, 1999). This may help to explain increases in sediment inputs on similar shelf deposits (e.g. Southern Washington/Northern Oregon (Twitchell and Cross, 2001). Such an increase in sediment supply could have compensated for increased loss from the shelf or enhanced sediment bypassing through canyons during lower sea level. Interestingly, this reconstruction of transgressive clinoform development does not require a fall in sea level as suggested for other systems (Fernandez-Salas et al., 2003).

5.6. Abrupt change ca. 11.5 ka

We ascribe the abrupt lithological transition from coarse, shell-rich sands and gravels to massive silt in our cores along >15 km of the outer shelf to the 11.5 ka MWP-1B drowning event. Based on the average accretion rates derived from ^{14}C ages of shells in the basal shallow-marine facies (Fig. 8, Table 1), this lithologic transition occurs at 11.4 ± 0.2 ka. The change in lithology ca. MWP-1B is consistent with rapid (1) drowning and decrease in near-bed shear stresses and (2) landward relocation of sediment inputs that would have occurred as the shoreline transgressed >2–3 km landward up and over the stepped R1 erosion surface. Sea-level reconstructions show that at the time the basal unit was deposited (15–11.5 ka), water depth (accommodation space) was 8–15 m near our core sites, while immediately following MWP-1B (the age of the

lithologic contact), water depth rapidly increased to ~50 m. This depth is consistent with the lower wave energy and the depth where a transition from sand to silt is observed on the shelf today (Fig. 7). In core 15, an earlier transition (12.6 ka) may represent localized change in depositional energy along line 309 (Figs. 1, 5).

5.7. *Role of time, topography and accommodation space on sediment accumulation*

A relatively simple model of the duration of time available for sediment accumulation during postglacial transgression on the central California shelf lends support to a postglacial origin for the mid-shelf deposit. Initial sea-level inundation for any depth on the shelf or R1 surface can be determined using a sea-level curve lookup table and accounting for uplift (Fig. 12). Correcting that shelf position for uplift over the duration of time it has been inundated, followed by a second consult of the eustatic sea level curve, provides a means of calculating the time of initial inundation of the shelf prior to uplift. Fig. 13(A) shows the timing of sea-level inundation across the central California shelf, assuming (1) the erosion surface (R1) is the Pleistocene–Holocene erosion surface, and (2) R1 experienced 1 mm/yr of uplift through time. This reconstruction of relative sea-level history provides a maximum age for postglacial marine deposition (i.e. deposition of the basal shallow-marine facies observed in cores and seismic reflection data). This model suggests that much of the shelf was inundated by ~11 ka and the present position of the shoreline was reached by sea level ~8–9 ka along most of the coast. If this last point is correct, littoral processes on the inner Santa Cruz shelf have operated 2–3 kyr longer than on stable coasts where sea level peaked ~6 ka (Bard et al., 1990; Peltier, 1994; Pirazzoli, 1991).

Dividing the deposit thickness (isopach map of Fig. 6) by shelf age (Fig. 13(A)) provides an estimate

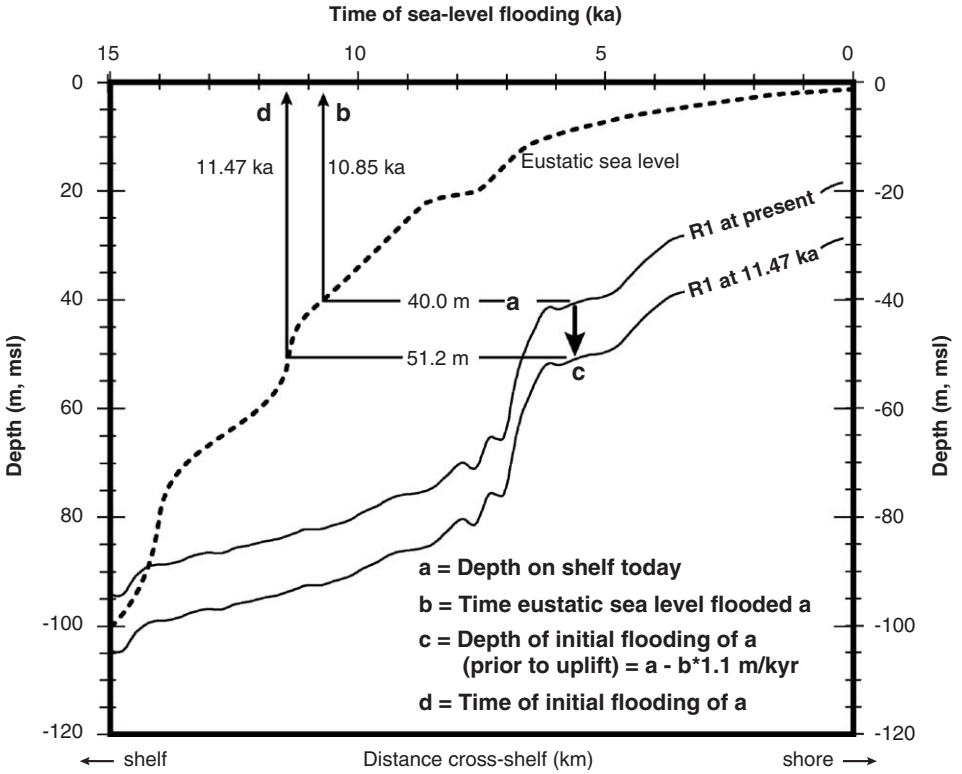

Fig. 12. Diagram showing method of determining initial sea-level inundation age of shelf prior to uplift. A position on the shelf today ($a = -40$ m) was inundated by eustatic sea level ca. 10.85 ka (b). Adjusting this depth for 10.85 kyr of uplift at the rate of 1.1 m/kyr we calculate the initial depth of flooding to be −51.20 m (c). The corresponding time of initial flooding (11.47 ka) then can be read off of the sea-level curve (d).

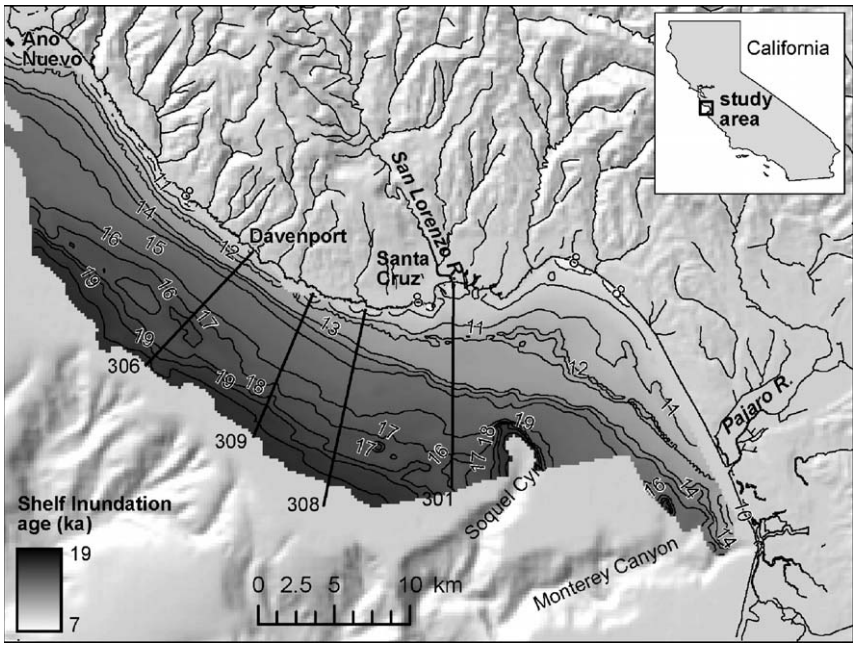

(A)

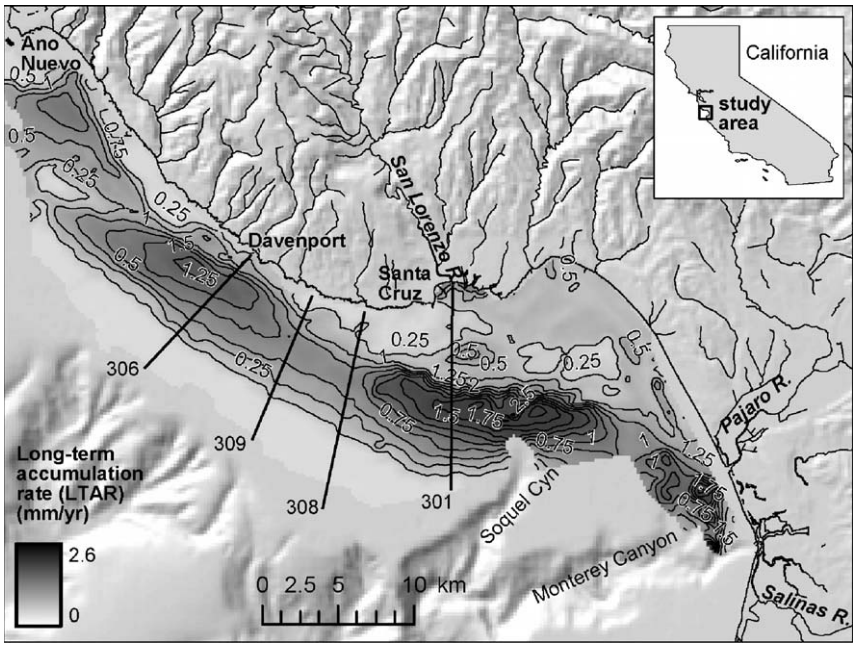

(B)

Fig. 13. (A) Map showing initial flooding age of shelf. This age provides a maximum age for deposition of marine sediments on the mid-shelf and a basis for calculating long-term sedimentation history. (B) Long-term accumulation rates (LTARs) across the mid-shelf deposit calculated by dividing deposit thickness (Fig. 6) by shelf inundation age (Fig. 13(B)). LTARs are minimum rates as deposition likely lagged an uncertain period of time behind sea-level inundation.

of long-term accumulation rates (LTARs) across the mid-shelf deposit (Fig. 13(B)) which are minimum rates since initial sedimentation likely lagged behind sea-level inundation, especially in the high-energy environment of central California. They can be compared to modern rates to test whether our

reconstructions are reasonable and whether the processes controlling sedimentation (e.g. accommodation space, uplift, sediment supply) are consistent with modern observations. Significant deviations between long-term and modern accumulation rates might elucidate possible variations in these processes and in sediment accumulation patterns or other environmental phenomena to explain the deposit origin. The calculated LTARs range between 0.01 and 2.60 mm/yr and are within the order of magnitude of and only slightly lower than modern rates based on ^{210}Pb that range 1.0–3.9 mm/yr (Lewis et al., 2002). They are greatest in mid-shelf depths near the base of the step in the pre-Holocene erosion surface (R1) and near the mouth of the Salinas River, consistent with modern observations, and reflect the importance of time, antecedent topography, and accommodation space on sediment accumulation across the shelf over long timescales.

A cross-section along Line 301 illustrates the importance of adequate accommodation space on sediment accumulation in two dimensions (Fig. 14). Fig. 14(A) shows the duration of time that each position of the surface (R1) along Line 301 spent within the depths that fine sand and silt are deposited today. This model of accommodation space accounts for uplift since initial shelf inundation (Fig. 13(A)) and variations in accommodation space resulting from changing position of sea level over the irregular stepped topography of surface R1. Fig. 14(B) shows the measured thickness of the mid-shelf deposit and the strong correlation between it and the duration of time for accommodation of fine sediment accumulation lends support for a postglacial origin of the entire mid-shelf deposit. The shape of the accommodation space curve and resulting deposit is controlled by the combined influence of the antecedent stepped morphology, uplift, and the episodic behavior of eustatic sea-level history.

A modern ^{14}C age of shell material buried at 50 cm within the silt drape (core 9) indicates that modern sedimentation and mixing occurs near the seaward edge of the mudbelt (Table 1, Fig. 2 and 6), consistent with ^{210}Pb analyses of recent sediment

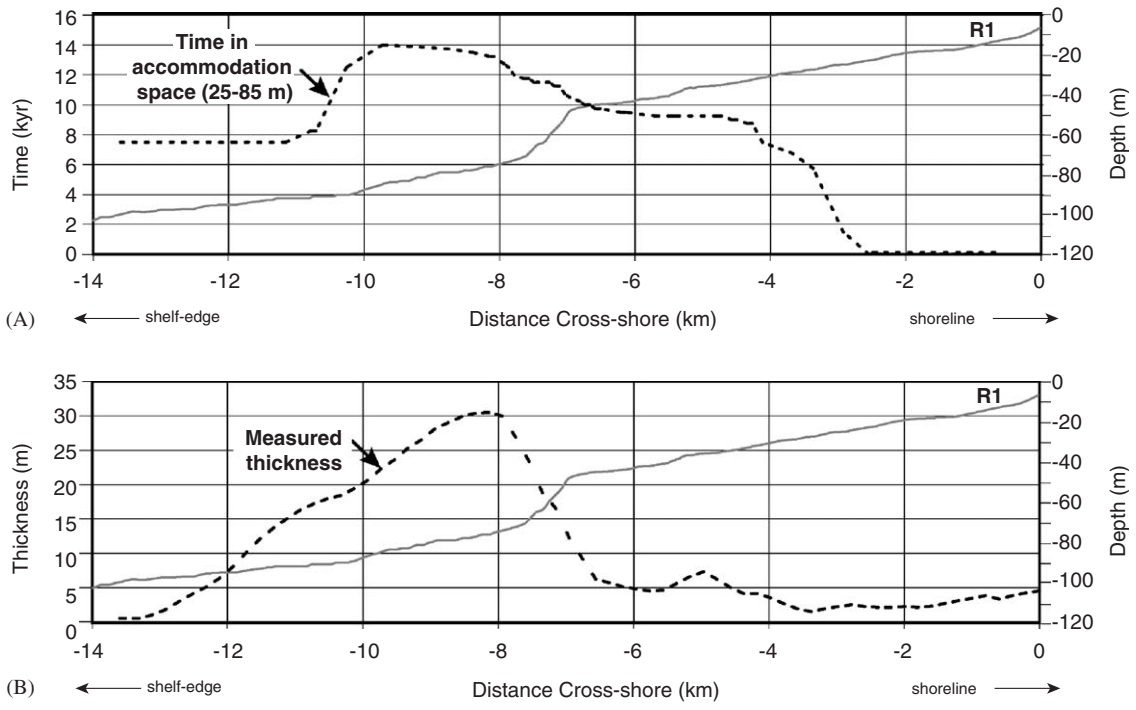

Fig. 14. (A) Plot of the duration of time that accommodation space for deposition of fine materials (fine sands and silt, today found between 25 and 85 m, Fig. 7) relative to the erosion surface (R1) along seismic line 301. (B) Plot of the measured mid-shelf deposit thickness along line 301 relative to R1. A peak of ~14 kyr in duration within the 25–85 m accommodation zone near the base of the erosional step provides a first-order prediction of the maximum mid-shelf deposit thickness.

accumulation across the mudbelt (Lewis et al., 2002). This upper 50-cm thick unit of the 50-km long, 5-km wide mudbelt offshore of Santa Cruz and the Salinas River contains 125,000,000 m^3, a volume representing ~70 yr of accumulation given the estimated modern rate of silt/clay input to the shelf of 1,750,000 m^3/yr (Eittreim et al., 2002b). This is a relatively short time and is consistent with the modern shell found in our study that suggests the upper portion of the mudbelt can be explained by modern sediment inputs and accumulation. These results also indicate, however, that modern sedimentation rates are significantly greater than those that formed the rest of the silt drape and mid-shelf sediment body. The silt drape is likely much older than 420–840 yr which would be calculated if the 3–6 m thick drape accumulates 50 cm every 70 yr. In addition, the basal ages of the deposit shown in this study (15,000–14,000 yr BP) are significantly older than a 3273 yr BP age derived by dividing the deposit volume (3.6×10^6 m^3) by the annual sediment accumulation rate that occurs over the mudbelt today (1,100,000 m^3/yr, Eittreim et al., 2002b; Lewis et al., 2002). This provokes questions regarding the fate of sediment reaching the shelf, processes that can explain the discrepancy between modern and past rates and patterns of sediment accumulation, and whether human activities are altering sedimentation on the seafloor as suggested by Paull et al. (2002).

6. Summary

Analyses of high-resolution shallow seismic reflection and sedimentologic data from cores and surface samples suggest that an extensive 3.6 km^3 (30-m thick) sediment body on the central California continental shelf likely formed during the postglacial transgression, beginning about 15 ka. An abrupt change in depositional environment occurred at ~12–11 ka after accumulation of a shallow basal lag that left outer and mid-shelf centers of accumulation far from their terrestrial sediment sources and in deep, calmer water where transport processes weakened. In the latter portion of the transgression, uplift rates as great as and sometimes greater than rates of sea-level rise brought the middle and inner shelf into the depths actively reworked by waves and currents forcing progradation of mid-shelf sediments. A model is proposed that describes how extensive progradation and delta-like clinoforms developed in response to the unique interaction of modest sediment supply and uplift, episodic and variable sea-level history, and a complex stepped antecedent substrate that immediately followed Meltwater Pulse 1B (11.5 ka) and lasted until ~6 ka. These conditions may have temporarily promoted progradation over back stepping despite sea-level transgression. An alternative model for the formation of the clinoform wedge is that progradation occurred during MIS 3 sea-level fall and preservation of the clinoform wedge was high during the postglacial transgression, possibly because of the stepped antecedent topography of the shelf.

Acknowledgements

This work was conducted as part of a postdoctoral research opportunity at the US Geological Survey and was supported in part by Office of Naval Research Grant N00014-99-F007. We recognize the forthcoming efforts of Pat Hart, Jon Childs, Ray Sliter, Josh Logan and Gerry Hatcher (USGS) and Gretchen Zwart (UC Santa Cruz) in assisting with seismic data processing and GIS, Stewart Fallon of the Center for Accelerator Mass Spectrometry at Lawrence Livermore Laboratories for radiometric analyses, and Kevin Orzech (USGS) for help in sediment-core lithologic analyses. We thank Jodi Harney, Jane Reid, and Noah Snyder of the USGS and Doug Inman of SCRIPPS Institute of Oceanography for constructive and engaging discussions. This manuscript benefited by the constructive reviews of Roberto Anima, Edward Clifton (USGS), and Marina Rabinaeu (IFREMER, France).

References

Anderson, R.S., 1994. Evolution of the Santa Cruz Mountains, California, through tectonic growth and geomorphic decay. Journal of Geophysical Research 99, 20161–20180.

Anderson, R., Densmore, A., Ellis, M., 1999. The generation and degradation of marine terraces. Basin Research 11, 7–19.

Anima, R., Eittreim, S., Edwards, B., Stevenson, A., 2002. Nearshore morphology and late Quaternary geologic framework of the northern Monterey Bay Marine Sanctuary, California. Marine Geology 181, 35–54.

Bard, E., Hamelin, B., Fairbanks, R., Zindler, A., 1990. Calibration of the 14-C timescale over the past 30,000 years using mass spectrometric U-Th ages from Barbados corals. Nature 345 (405–409).

Best, T.C., 1990. A Sediment Budget for the Santa Cruz Littoral Cell. University of California, Santa Cruz, CA, (55pp).

Best, T.C., Griggs, G.B., 1991. A sediment budget for the Santa Cruz littoral cell, California. In: Osborne, R.H. (Ed.), From Shoreline to Abyss. Society of Economic Paleontologists and Mineralogists, pp. 35–50.

Bradley, W., Griggs, G., 1976. Form, genesis, and deformation of central California wave-cut platforms. Geological Society of America Bulletin 87, 433–449.

Cattaneo, A., Steel, R., 2003. Transgressive deposits: a review of their variability. Earth-Science Reviews 62 (3–4), 187–228.

Chin, J.L., Clifton, H.E., Mullins, H.T., 1988. Seismic stratigraphy and late Quaternary shelf history, south-central Monterey Bay, California. Marine Geology 81, 137–157.

Edwards, B.D., 2002. Variations in sediment texture on the northern Monterey Bay National Marine Sanctuary continental shelf. Marine Geology 181, 83–100.

Eittreim, S.L., Noble, M., 2002. Seafloor geology and natural environment of the Monterey Bay National Marine Sanctuary. Marine Geology 181 (1–2).

Eittreim, S.L., Anima, R.J., Stevenson, A.J., 2002a. Seafloor geology of the Monterey Bay area shelf. Marine Geology 181, 3–34.

Eittreim, S.L., Xu, J.P., Noble, M., Edwards, B.D., 2002b. Towards a sediment budget for the Santa Cruz shelf. Marine Geology 181, 235–248.

Fairbanks, R., 1990. The age and origin of the "Younger Dryas climate event" in Greenland ice cores. Paleoceanography 5 (6), 937–948.

Fernandez-Salas, L., et al., 2003. High-resolution architecture of late Holocene highstand prodeltaic deposits from southern Spain: the imprint of high-frequency climatic and relative sea-level changes. Continental Shelf Research 23 (11–13), 1037–1054.

Fletcher, C.H.I., Sherman, C.E., 1995. Submerged shorelines on Oahu, Hawaii: Archive of episodic transgression during the deglaciation? Journal of Coastal Research (Special Issue 17), 141–152.

Frignani, M., et al., 2005. Fine-sediment mass balance in the western Adriatic continental shelf over a century time scale. Marine Geology 222–223, 113–133.

Greene, H.G., 1977. Geology of the Monterey Bay region. US Geology Survey Open File Report no. 77-718, 347pp.

Greene, H.G., Maher, N.M., Paull, C.K., 2002. Physiography of the Monterey Bay National Marine Sanctuary and implications about continental margin development. Marine Geology 181 (1–3), 55–82.

Hampson, G.J., Storms, J.E.A., 2003. Geomorphological and sequence stratigraphic variability in wave-dominated, shoreface-shelf parasequences. Sedimentology 50 (4), 667–701.

Hampton, M.A., Karl, H.A., Murray, C.J., 2002. Acoustic profiles and images of the Palos Verdes margin: implications concerning deposition from the White's Point outfall. Continental Shelf Research 22 (6–7), 841–857.

Harris, C., Wiberg, P., 1997. Approaches to quantifying long-term continental shelf sediment transport with an example from the Northern California STRESS mid-shelf site. Continental Shelf Research 17 (11), 1389–1418.

Hicks, D.M., Inman, D.L., 1987. Sand dispersion from an ephemeral river delta on the central California coast. Marine Geology 77, 305–318.

Hughes, T.P., et al., 2003. Climate change, human impacts, and the resilience of coral reefs. Science 301 (5635), 929–933.

Inman, D., Jenkin, S., 1999. Climate change and the episodicity of sediment flux of small California rivers. Journal of Geology 107, 251–270.

Jackson, J.B.C., et al., 2001. Historical overfishing and the recent collapse of coastal ecosystems. Science 293 (5530), 629–637.

Kennedy, G., Lajoie, K., Wehmiller, J., 1982. Aminostratigraphy and faunal correlations of late Quaternary marine terraces, Pacific Coast, USA. Nature 299 (5883), 545–547.

Labaune, C., et al., 2005. Seismic stratigraphy of the Deglacial deposits of the Rhone prodelta and of the adjacent shelf. Marine Geology 222–223, 299–311.

Lajoie, K., Ponti, D., Powel, C., Mathieson, S., Sarna-Wjcicki, A., 1991. Emergent marine strandlines and associated sediments, coastal California: a record of Quaternary sea-level fluctuations, vertical tectonic movements, climate changes, and coastal processes. In: Morrison, R. (Ed.), Quaternary Nonglacial Geology: Conterminous United States. Geological Society of America, Geology of North America, Boulder, CO, pp. 190–214.

Lea, D., Martin, P., Pak, D., Spero, H., 2002. Reconstructing a 350 ky history of sea level using planktonic Mg/Ca and oxygen isotope records from a Cocos Ridge core. Quaternary Science Reviews 21, 283–293.

Lewis, R.C., et al., 2002. Accumulation rate and mixing of shelf sediments in the Monterey Bay National Marine Sanctuary. Marine Geology 181, 157–169.

Liu, T., Broecker, W., Bell, J., Mandeville, C., 2000. Terminal Pleistocene wet event recorded in rock varnish from Las Vegas Valley, Southern Nevada. Paleogeography, Paleoclimatology and Paleocecology 161, 423–433.

Mullins, H.T., Nagel, D.K., Dominguez, L.L., 1985. Tectonic and eustatic controls of late Quaternary shelf sedimentation along the central California (Santa Cruz) continental margin: high-resolution seismic stratigraphic evidence. Sedimentary Geology 45, 327–347.

Nagel, D.K., Mullins, H.T., 1983. Late Cenozoic offset and uplift along the San Gregorio fault zone, Central California continental margin. Pac. Sect. Soc. Econ. Paleontol. Mineral. Symp., vol. Tectonics and Sedimentation Along Faults of the San Andreas System, Los Angeles, CA., pp. 91–103.

Neill, C.F., Allison, M.A., 2005. Subaqueous deltaic formation on the Atchafalaya Shelf, Louisiana. Marine Geology 214 (4), 411–430.

Nittrouer, C., 1999. STRATAFORM: overview of its design and synthesis of its results. Marine Geology 154, 3–12.

Nittrouer, C.A., Sternberg, R.W., 1981. The formation of sedimentary strata in an allochthonous shelf environment: The Washington continental shelf. Marine Geology 42 (1–4), 201–232.

Paull, C.K., Greene, H.G., Ussler, W., Mitts, P.J., 2002. Pesticides as tracers of sediment transport through Monterey Canyon. Geo-Marine Letters 22, 121–126.

Peltier, W., 1994. Ice age paleotopography. Science 265, 195–201.

Perg, L.A., Anderson, R.S., Finkel, R.C., 2001. Use of a new 10 Be and 26 Al inventory method to date marine terraces, Santa Cruz, California, USA. Geology 29, 879–882.

Perg, L.A., Anderson, R.S., Finkel, R.C., 2003. Use of cosmogenic radionuclides as a sediment tracer in the Santa Cruz littoral cell, California, United States. Geology 31, 299–302.

Pirazzoli, P., 1991. World Atlas of Holocene Sea-Level Changes. Elsevier, New York, 300pp.

Pirmez, C., Pratson, L., Steckler, M., 1998. Clinoform development by advection–diffusion of suspended sediment: modeling and comparison to natural systems. Journal of Geophysical Research 103 (B10), 24,141–24,157.

Reid, J., et al., 2002. usSEABED: towards unifying knowledge of geological controls on benthic habitats. In: Symposium on Effects of Fishing Activities on Benthic Habitats: Linking Geology, Biology, Socioeconomics, and Management, Tampa, FL.

Rhode, D., 2002. Early Holocene Juniper woodland and chaparral taxa in the central Baja California Peninsula, Mexico. Quaternary Research 57, 102–108.

Robinson, S., Thompshon, G., 1981. Radiocarbon corrections for marine shell dates with application to southern Pacific Northwest Coast prehistory. Syesis 14, 45–57.

Smith, R., Carlton, J., 1975. Light's Manual: Intertidal Invertebrates of the Central California Coast. University of California Press, Berkeley, 716pp.

Sommerfield, C.K., Lee, H.J., 2004. Across-shelf sediment transport since the Last Glacial Maximum, southern California margin. Geology 32 (4), 345–348.

Sommerfield, C.K., Nittrouer, C.A., 1999. Modern accumulation rates and a sediment budget for the Eel shelf: a flood-dominated depositional environment. Marine Geology 154 (1–4), 227–241.

Sommerfield, C.K., Drake, D.E., Wheatcroft, R.A., 2002. Shelf record of climatic changes in flood magnitude and frequency, north-coastal California. Geology 30 (5), 395–398.

Storlazzi, C.D., Jaffe, B.E., 2002. Flow and sediment suspension events on the inner shelf of central California. Marine Geology 181, 195–213.

Storms, J.E.A., 2003. Event-based stratigraphic simulation of wave-dominated shallow-marine environments. Marine Geology 199 (1–2), 83–100.

Stuiver, M., Reimer, P., 1993. Extended C-14 data-base and revised Calib 3.0 C-14 age calibration program. Radiocarbon 35 (1), 215–230.

Stuiver, M., Reimer, P.J., Bard, E., Beck, J.W., Burr, G.S., Hughen, K.A., Kromer, B., McCormac, G., Van der Plicht, J., Spurk, M., 1998. INTCAL98 radiocarbon age calibration, 24,000–0 cal BP. Radiocarbon 40 (3), 1041–1083.

Sunamura, T., 1992. Geomorphology of Rocky Coasts. Oxford University Press, Trenhaile, 384pp.

Suter, J., Berryhill, H., 1985. Late Quaternary shelf-margin deltas, Northwest Gulf of Mexico. American Association of Petroleum Geologists Bulletin 69 (1), 77–91.

Swift, D., Oertel, G., Tillman, R., Thorne, J. (Eds.), 1991. Shelf Sand and Sandstone Bodies: Geometry, Facies and Sequence Stratigraphy. Blackwell Scientific Publications, Oxford, (532pp).

Thornton, E.B., Egley, L.A., Sallenger, A., Parsons, R., 2003. Erosion in Southern Monterey Bay during the 1997–98 El Niño. In: Proceedings of the Fifth International Symposium on Coastal engineering and Science of Coastal Sediment Processes, Clearwater Beach, FL, 18–23 May, pp. 1–10.

Trincardi, F., Field, M., 1991. Geometry, lateral variation, and preservation of downlapping regressive shelf deposits: eastern Tyrrhenian Sea margin, Italy. Journal of Sedimentary Petrology 61 (5), 775–790.

Twitchell, D., Cross, V., 2001. Holocene evolution of the southern Washington and northern Oregon shelf and coast: geologic discussion and GIS data release. USGS Open-File Report 01-076.

Van Wagoner, J., et al., 1988. An overview of the fundamentals of sequence stratigraphy and key definitions. In: Wilgus, C., et al. (Eds.), Sea-Level Changes—An Integrated Approach. Society of Economic Paleontologists and Mineralogists, Tulsa, (407pp).

Wheatcroft, R.A., Borgeld, J.C., 2000. Oceanic flood deposits on the northern California shelf: large-scale distribution and small-scale physical properties. Continental Shelf Research 20 (16), 2163–2190.

Wiberg, P., Drake, D., Harris, C., Noble, M., 2002. Sediment transport on the Palos Verdes shelf over seasonal to decadal time scales. Continental Shelf Research 22 (6–7), 987–1004.

Xu, J.P., Noble, M., Eittreim, S.L., 2002. Suspended sediment transport on the continental shelf near Davenport, California. Marine Geology 181, 171–193.